Supporting Information

Bacterial 16S metabarcoding methods

The initial PCR mixture amplifying community bacterial DNA used 1X AccuPrime SuperMix II (Invitrogen, Eugene, OR, USA), 0.5 μM (each) forward and reverse primers, ~5 ng DNA, and DNase/RNase-free water to a final volume of 20 μL. The PCR profile consisted of an initial denaturation step at 95°C for 2 min, followed by 30 cycles of 95°C for 15 s, 55°C for 15 s, and 68°C for 40 s and a final elongation step at 68°C for 4 min.

Dual indices and sequencing adapters were attached to the amplicons in an additional PCR reaction using a Nextera XT v2 index kit (Illumina Inc.). Five microliters of the first PCR product, 12 μL AccuPrime SuperMix II (Invitrogen, Eugene, OR, USA), 2 μL of each Nextera i7 and i5 index primer, and DNase/RNase-free water were mixed to a final volume of 28 μL in the second PCR. The PCRII profile consisted of an initial denaturation step at 95°C for 2 min, followed by 5-7 cycles of 95°C for 10 s, 55°C for 20 s, and 68°C for 20 s and a final elongation step at 68°C for 5 min.

Prior to sequencing, the final PCR products were visualized on a 2% agarose gel electrophoresis, pooled equimolar (or of each blank at the volume of the least concentrated sample), and purified with a 0.7X ratio of Agencourt AMPure bead purification (Beckman Coulter, Inc, Brea, California), following the manufacturer's protocol. Final concentrations were measured on a Qubit™ and library quality was verified on the 2200 TapeStation prior to sequencing on an Illumina MiSeq platform using 250PE chemistry.

Supplementary Figures:

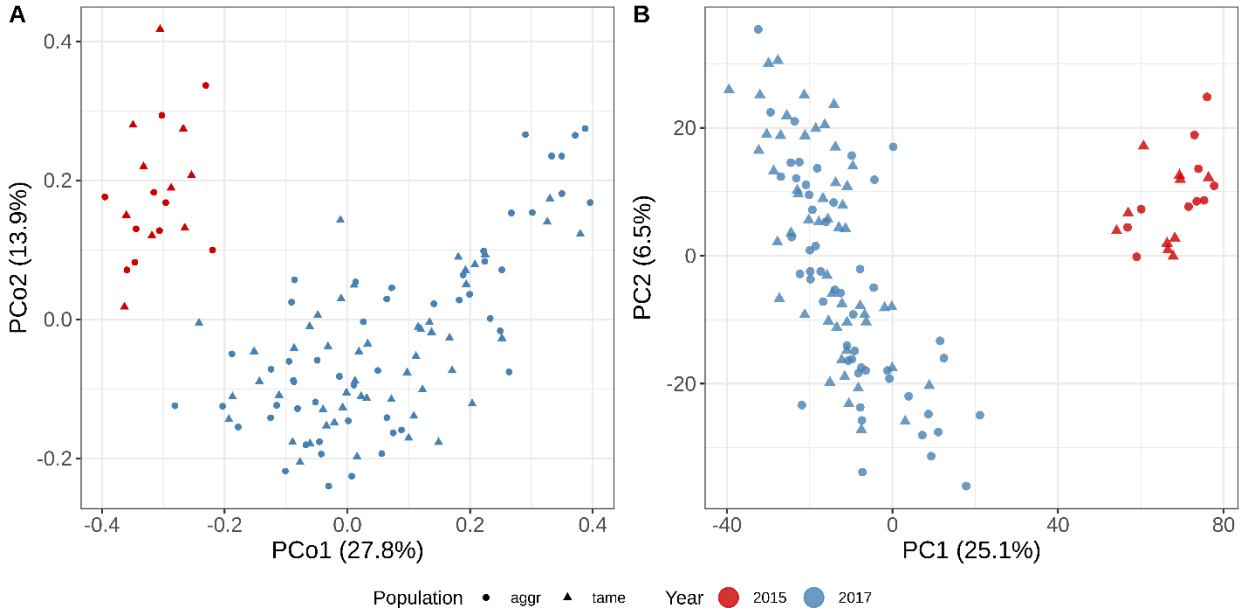

Supplementary Fig. 1. Ordination of the gut microbial communities of foxes indicates strong batch effects between collection years. A) Principle coordinate analysis (PCoA) of the Bray-Curtis dissimilarity matrices of the relative abundance of bacterial 16S ASV sequence data. **B)** Principle component analysis of the log-ratios of the number of reads mapped to each of the MAGs per fox sample. Both ordination plots show clear batch effects between the 2015 data (n=20; frozen -20°C) and the 2017 data (n=103; preserved in RNAlater).

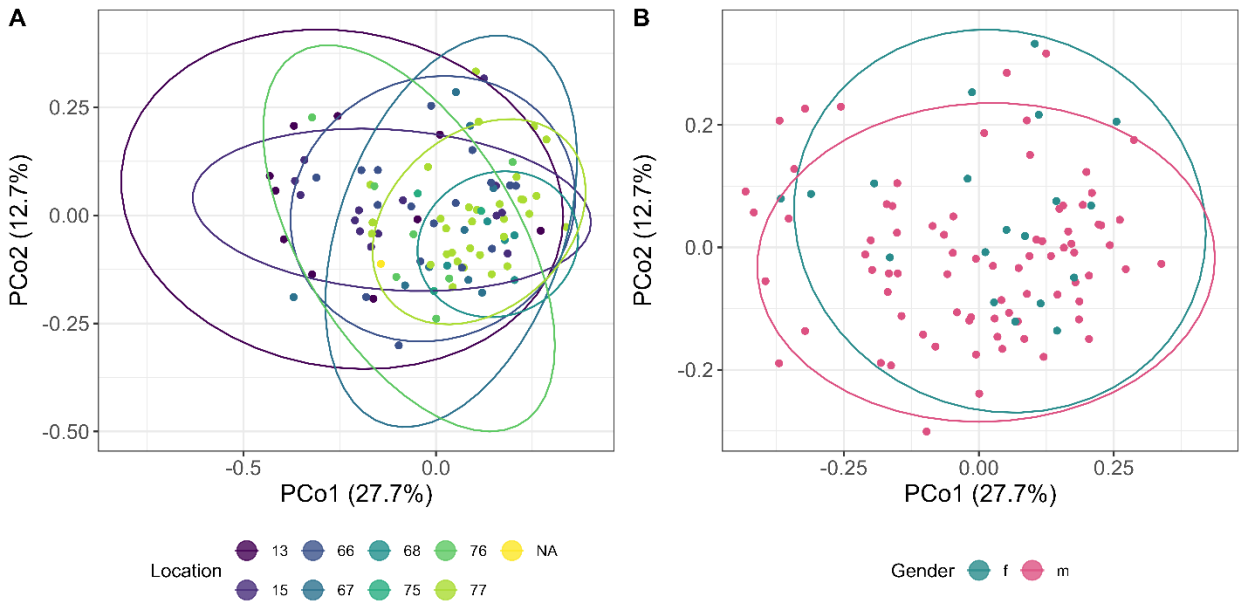

Supplementary Fig. 2. Ordination of the gut microbial communities of foxes (n=103) indicates no clustering among A) fox housing sheds (located on the same farm in near proximity to one another) nor B) between male (m) and female (f) foxes. Plots represent the principle coordinate analysis (PCoA) of the Bray-Curtis dissimilarity matrices of the relative abundance of bacterial 16S ASV sequence data.

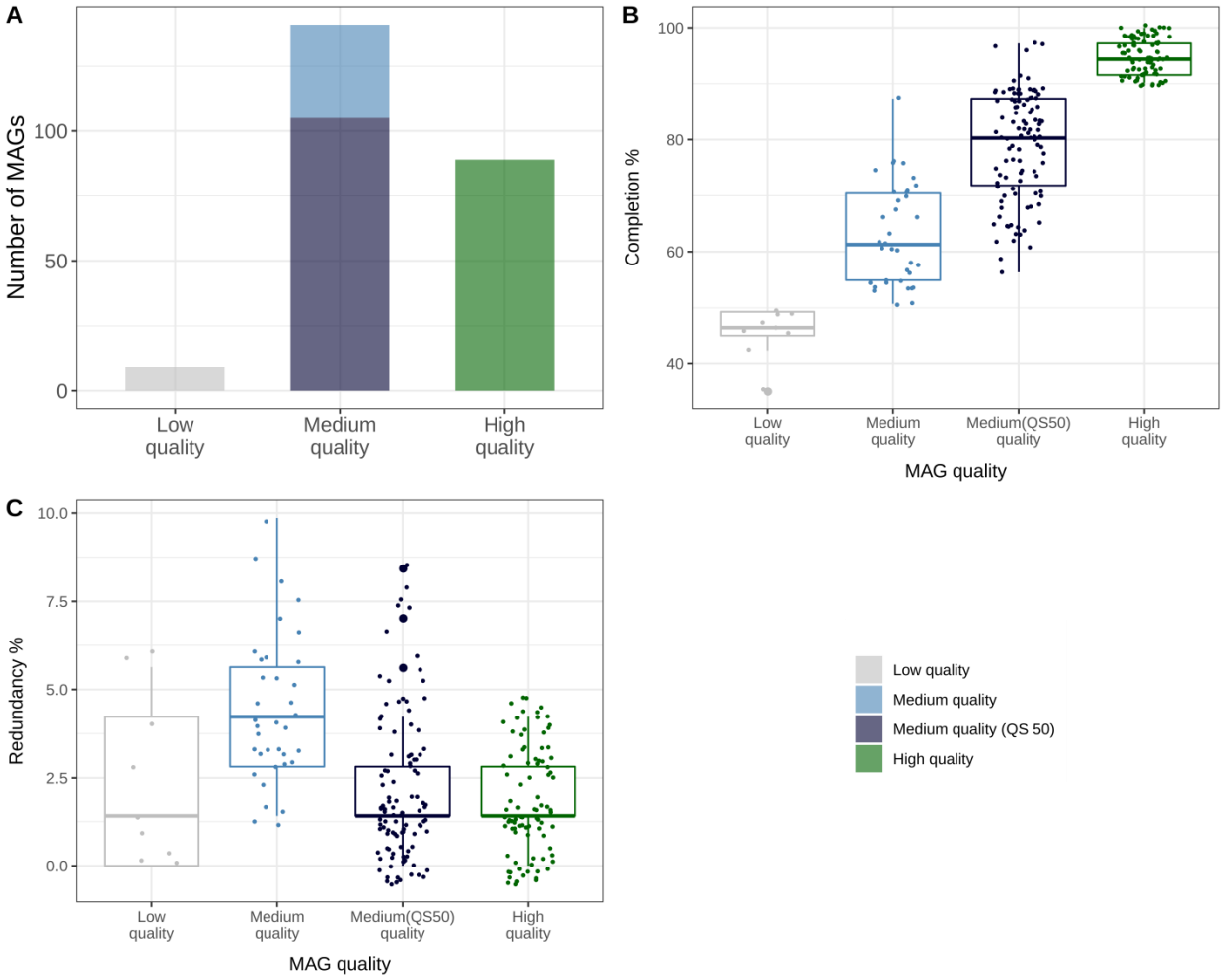

Supplementary Fig. 3. Quality metrics estimated by Anvi'o for the 237 fox bins generated by a manual binning strategy within the anvi'o framework. Low quality BINs were removed from the analyses. **A)** Number of bins recovered according to the level of genome completeness and redundancy. Box and whisker plots for the **B)** percentage of completion and **C)** percentage of redundancy for each bin grouped by the quality standard of the draft genome. QS = completeness – (5 × contamination).

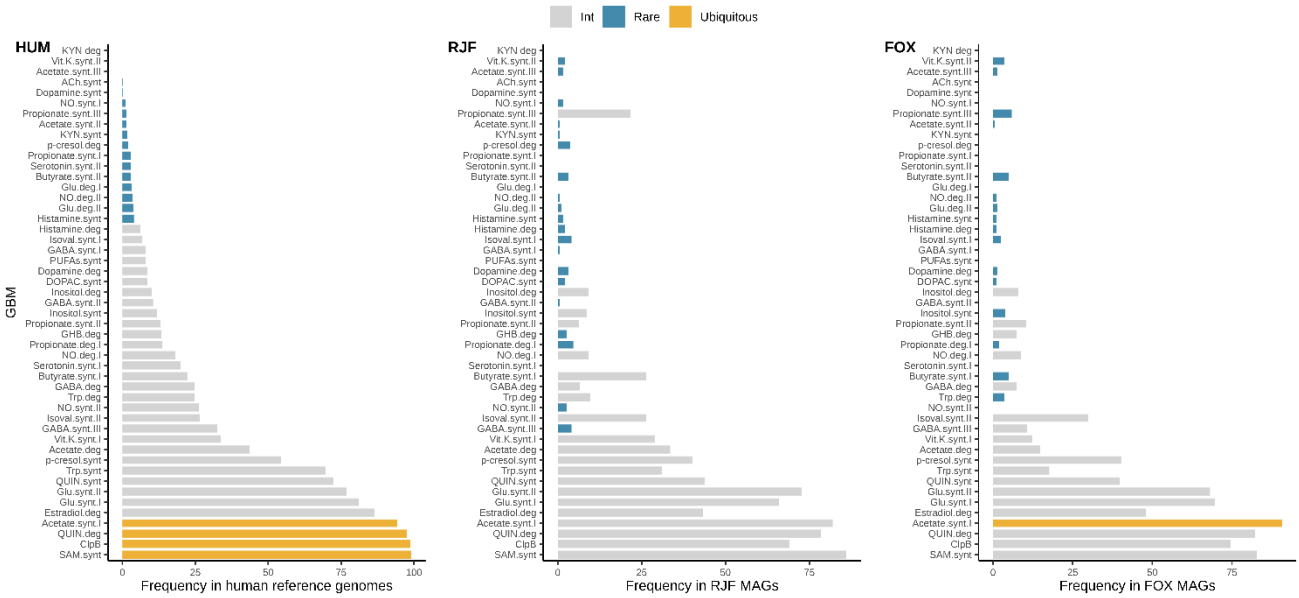

Supplementary Fig. 4. Comparison of gut-brain-module (GBM) distribution in human, red junglefowl and fox microbial genomes. GBM detection frequency in **HUM)** human gut-associated microbial reference genomes (n = 532) drawn from (Valles-Colomer *et al.*, 2019) and previously used to validate the GBM framework, **RJF)** red junglefowl MAGs (n=194) identified from fecal samples in previously published study (Puetz et al., 2021) and **FOX)** fox MAGs (n=237) identified from fecal samples in current study. Rare (< 5% of genomes) and ubiquitous GBMs (> 90% genomes) are highlighted, while others are in grey. Figure modified from (Valles-Colomer et al., 2019 [1]).

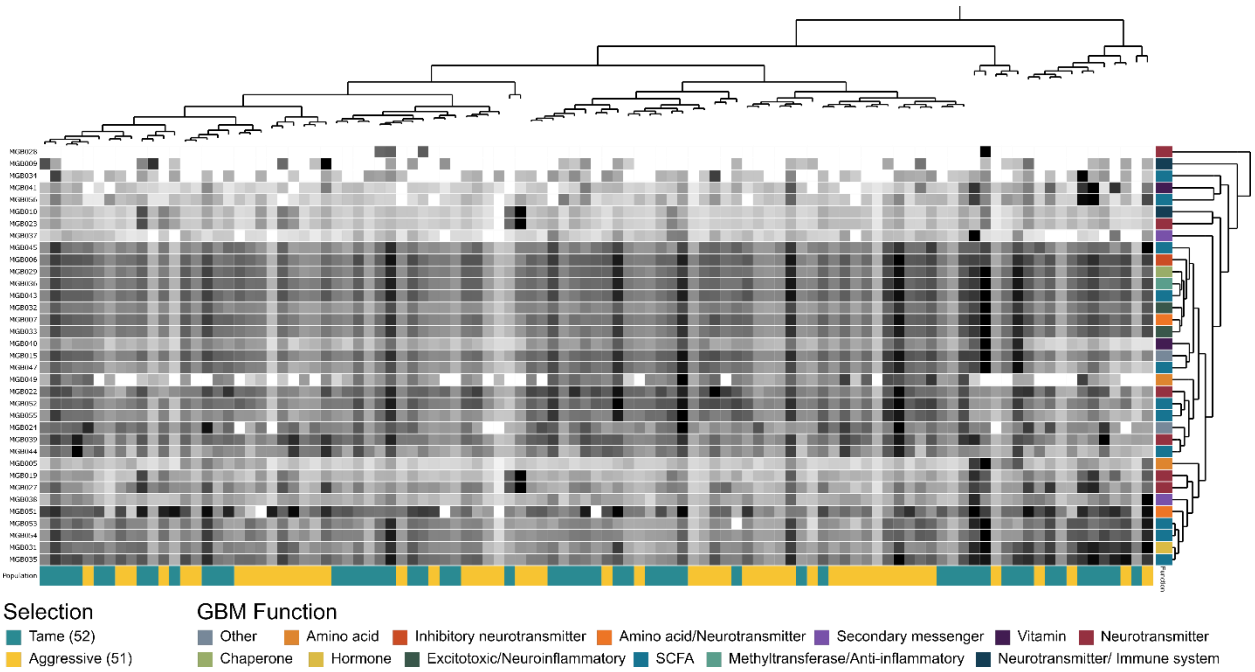

Supplementary Fig. 5. Gut-brain module (GBM) distribution in fox metagenomes. Heatmap of the $\log_{10}$ frequency of 35 GBMs detected in 102 fecal metagenomes of silver fox selected for tame and aggressive behaviors towards humans. Clustering of GBMs and metagenomes is based on GBM frequency (Euclidean distance and ward linkage), and the data were visualized using anvi'o.

Supplementary References

1. Valles-Colomer, M. et al. The neuroactive potential of the human gut microbiota in quality of life and depression. Nat. Microbiol. 4, 623–632 (2019).